Delayed Signal Propagation via CA2 in Rat Hippocampal Slices Revealed by Optical Recording

YUKO SEKINO, KUNIHIKO OBATA, MANABU TANIFUJI, MAKOTO MIZUNO, AND JIN MURAYAMA
Precursory Research for Embryonic Science and Technology, Japan Science and Technology Corporation, Laboratory of Neurochemistry, National Institute for Physiological Sciences, Okazaki 444; Department of Information and Communication Engineering, Tamagawa University, Machida, Tokyo 194; and Fujifilm Microdevices, Miyagi 981-34, Japan

Sekino, Yuko, Kunihiko Obata, Manabu Tanifuji, Makoto Mizuno, and Jin Murayama. Delayed signal propagation via CA2 in rat hippocampal slices revealed by optical recording. *J. Neurophysiol.* 78: 1662–1668, 1997. Signal propagation from mossy fibers to CA1 neurons was investigated in rat hippocampal slices by a combination of electrical and optical recordings. The slices were prepared by oblique sectioning of the middle part of the hippocampus to preserve fiber connections. The mossy fibers were stimulated to induce population spikes (PSs) and excitatory postsynaptic potentials in the middle part of the CA1 region. Latencies of maximal PSs in CA1 varied widely among slices; they ranged from 7 to 13.5 ms, with two maxima at 9 and 11.5 ms. The fastest PSs probably are evoked by the Schaffer collaterals that connect the CA3 and CA1 regions in the well-known trisynaptic circuit. However, the slower PSs suggest the existence of additional delayed inputs. To determine the source of the delayed input, slices were stained with a voltage-sensitive dye, RH482, and the optical signals relevant to membrane potential changes were detected by a high-resolution optical imaging system. Optical recording of responses to mossy fiber stimulation indicated two distinct types of signal propagation from CA3 to CA1. In preparations evincing the fast type of propagation, signals spread to CA1 within 7.2 ms after the mossy fiber stimulation. During such propagation, activity flowed directly from CA3 to the stratum radiatum of CA1. Other preparations illustrated slow signal propagation, in which optical signals were generated in CA2 before spreading to CA1. During such slow signal transmission, activity persisted in CA2 and its surrounding area for 3 ms before propagating to the strata radiatum and oriens in CA1. In such cases, CA1 activity was detected within 10.8 ms of mossy fiber stimulation. In some slices, a mixture of the fast and slow propagation patterns was observed, indicating that these two transmission modes can coexist. Our data reveal that CA2 neurons can transmit delayed excitatory signals to CA1 neurons. We therefore conclude that consideration of electrical signal propagation through the hippocampus should include flow through the CA2 region in addition to the traditional dentate gyrus–CA3–CA1 trisynaptic circuit.

INTRODUCTION

The hippocampus participates in memory formation (Scoville and Milner 1957; Zola-Morgan and Squire 1990; Zola-Morgan et al. 1986). Therefore neural circuits in the hippocampus must be fully elucidated to understand the neural mechanisms of memory formation. Most studies on synaptic transmission and plasticity (Alger and Teyler 1976; Schwartzkroin and Wester 1975; reviewed by Bliss and Collingridge 1993) are based on the trisynaptic circuit in the hippocampus (Andersen et al. 1971), which consists of the perforant path, granule cells, CA3 pyramidal cells, and CA1 pyramidal cells: the perforant path excites the granule cells in the dentate gyrus (DG), the mossy fibers from the granule cells excite the CA3 cells, and the Schaffer collaterals of CA3 axons excite the CA1 pyramidal cells. This circuit, however, may be an oversimplified view of intrahippocampal connections. Although the CA2 region is identified between the CA3 and CA1 regions (Lorente de Nó 1934; Tamamaki et al. 1988), participation of CA2 cells in hippocampal function has been ignored in most theoretical studies of CA3-CA1 connection. Usually, the CA2 region has been treated as a distal part of CA3 (Bernard and Wheal 1994). Focal axon bundle labeling (Amaral and Witter 1989) and single-cell labeling studies (Ishizuka et al. 1990; Tamamaki et al. 1988) have shown that CA3 and CA2 cells have many association fibers distributed more widely across the septotemporal axis than expected in the trisynaptic concept. These facts suggest that novel circuits, in addition to the trisynaptic circuit, contribute to intrahippocampal networks.

One of the reasons why polysynaptic connections in the hippocampus have not yet been fully elucidated is that widespread and prolonged information flow cannot be detected by conventional electrophysiological recording. Optical recording with voltage sensitive dyes is expected to overcome such drawbacks because it can monitor electrical activities in a larger area simultaneously and has been used for measuring spread of neural activity in various brain regions (Cinelli and Kauer 1992; Grinvald et al. 1981; Iijima et al. 1996; Konnerth et al. 1987; Tanifuji et al. 1994).

In the present study, we investigated propagation of neural activity from CA3 to CA1 in obliquely sectioned slice preparations in which intrahippocampal connections were well preserved, and we disclosed delayed propagation via CA2 in addition to rapid propagation via the Schaffer collateral pathway.

METHODS

Slice preparation

Adult Long-Evans male rats (200–250 g) were anesthetized with pentobarbital sodium (50 mg/kg ip), and the cerebrum was dissected out. After removal of the brain stem, the hemispheres were placed on the cutting stage of a rotor slicer (DM-1000, Dosaka EM), with the ventral surface of the hippocampus up, and embedded in low-melting-point agarose (Sea Plaque GTG agarose; FMC Bioproducts). The tissue was sliced (500 μm in thickness) at an angle of 30–45° to the long axis of the hippocampus. This

angle was selected because the plane was parallel to the alvear fibers that were on the surface of the tissue and the trisynaptic circuit (Andersen et al. 1971). The slices were obtained only from the middle part of the hippocampus and were preincubated for >1 h at 32°C in an interface-type reservoir perfused with Krebs-Ringer solution (pH 7.35) equilibrated with 95% O_2-5% CO_2. The solution contained (in mM) 124 NaCl, 5.0 KCl, 2.6 NaH_2PO_4, 2.0 $MgSO_4$, 2.0 $CaCl_2$, 26 $NaHCO_3$, and 10 glucose. After the preincubation, the slices were stained with a dye, RH482 (produced as NK3630 by Nippon Kankoh-Shikiso), at a concentration of 0.02% for 15 min before optical recording. The optical absorbance of this dye changes according to the membrane potential of neurons (Grinvald et al. 1980) but not in response to slow potential changes of glial origin (Konnerth et al. 1987). Each slice was mounted in a recording chamber placed on an inverted microscope (Axiovert, Zeiss), and perfused at 30–32°C with Krebs-Ringer solution at a rate of 0.5–1 ml/min. Subregions of the hippocampus in each slice were identified under a microscope. In particular, the CA2 region was identified as a ''hump'' region between the CA3 and CA1 regions. The pyramidal cell layer in CA2 was thicker than that in other regions and packed with larger but somewhat irregularly distributed cells (Haug 1974; Lorente de Nó 1934).

Electrophysiology

A bipolar tungsten electrode was placed on the hilus for stimulation of the mossy fibers. Stimuli were applied at a frequency of 0.2 Hz during acquisition of optical signals and otherwise at 0.1 Hz. Population spikes (PSs) and field excitatory postsynaptic potentials (EPSPs) were recorded in the cell body layer and stratum radiatum, respectively, with a 2- to 3-MΩ glass microelectrode filled with saline to monitor propagation of neural activities from mossy fibers to CA1 neurons. To confirm stable electrical responses during optical measurement, PSs were monitored in the middle part of CA1, just beyond the optical recording site, because the electrode in the light path disturbed imaging.

Optical measurement of membrane potential change

A 150-W halogen lamp was lit with a stabilized DC power supply. A heat absorption filter, an interference filter (wavelength 700 ± 30 nm), and a mechanical shutter were inserted in the light path between the light source and a condenser lens. Light was passed through the brain slice, collected by an objective lens (Plan-Apochromat ×5, numerical aperture 0.16, Zeiss), and focused in an optical recording system. The change in light absorption by RH482 was detected by a metal oxide (MOS) image sensor (9.0×9.0 mm^2, 128×128 pixels) (Ichikawa et al. 1993; Tanifuji et al. 1994) in a camera system (SD1001, Fujifilm Microdevices). Thus the sensor covered the hippocampal area of 1.8×1.8 mm^2 that extended from the hilus through the middle part of CA1.

Neural activity was recorded as a change in the intensity of the light passing through preparations stained with RH482. Membrane depolarization was measured as a decrease in the intensity of the light. The slice preparation was illuminated for only 680 ms in each acquisition to prevent dye bleaching. Any optical signal was not obtained from unstained preparations.

In each acquisition trial, 128 consecutive images were acquired at 0.6-ms intervals. Each image (I) was subtracted from an initial control image (I_0) in each pixel. This difference image ($\Delta I = I - I_0$) was amplified 400 times by the differential optoanalyzer system. $\Delta I/I$ values were between 0.03% and 0.15%. This was well over the limit of the detector in our system (0.01%). In each experiment, 16 trials were averaged to improve further the signal-to-noise ratio of the images. The intensity of electrical stimuli (duration 200 μs) was twice that required to evoke a maximal PS in CA1 (0.2–0.6 mA), which was determined with the use of stimulus-response curves. The images were displayed with pseudocolor intensity coding. A photograph of each slice (a real image) was taken to identify the site of the optical signals.

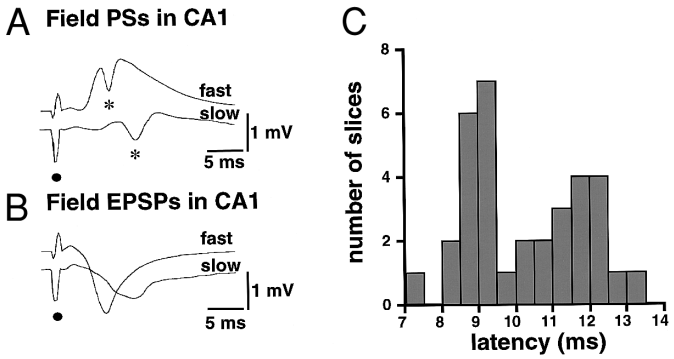

FIG. 1. Differences in latencies of field potentials in middle part of CA1 induced by maximal stimulation of mossy fibers in hilus. *A*: typical field population spikes (PSs) recorded in stratum pyramidale in 2 individual slices showing a short latency (8 ms, *top trace* shown as a fast PS) and a long latency (11.8 ms, *bottom trace* shown as a slow PS) induced by maximal stimulation (0.3 and 0.6 mA, respectively). *B*: field excitatory postsynaptic potentials (EPSPs) simultaneously recorded with PSs. A fast EPSP (*top trace*) and a slow EPSP (*bottom trace*) were recorded in stratum radiatum. *C*: latency histogram for PSs. Latency is defined as the time interval from stimulus (*A* and *B*, ●) to negative peak of PSs (*A*, ∗). Latencies were broadly distributed with 2 peaks between 7 and 13.5 ms ($n = 34$).

RESULTS

Electrophysiological studies suggested fast and slow pathway from CA3 to CA1

When the hippocampal formation was sliced transversely, as it is in most of electrophysiological investigations, stimulation of mossy fibers evoked PSs of pyramidal cells in CA3 and stimulation of the Schaffer/commissural collateral axons in the stratum radiatum evoked PSs in CA1. However, stimulation of mossy fibers in the hilus rarely produced PSs in CA1 ($n = 14$). On the other hand, when the tissue was sliced along the obliquely running alvear fibers, mossy fiber stimulation induced PSs in CA1 with a peak value of >1 mV in most cases ($n = 34$). The latency and the amplitude of PSs in each slice were stable during each experiment. PSs recorded in CA1, however, showed various latencies among slices (Fig. 1).

Two distinct types of PSs with different latencies from the stimulus (●) to the negative peaks (∗) are shown in Fig. 1*A*. The fast PS had an 8.0-ms latency and the slow PS had a 12.0-ms latency. EPSPs simultaneously recorded in the stratum pyramidale of the middle part of CA1 in the same slices also showed fast and slow initial slope (Fig. 1*B*). A trace of PS recorded in the cell layer is composed of the reversed-polarity EPSP and superimposed PS. The latencies of PSs corresponded well to those of EPSPs, and were easier to estimate than those of EPSPs. To clarify existence of two types of PSs in the stratum pyramidale of the middle part of CA1, we obtained a latency histogram from 34 slices (Fig. 1*C*). The latencies varied widely among slices; they ranged from 7 to 13.5 ms, with two maxima at 9 and 11.5 ms. Therefore the responses in CA1 were tentatively classified as fast and slow, respectively.

When PSs were recorded in the middle part of CA3, their latency was nearly constant among slices (3.0–4.5 ms).

Therefore the variation of the latencies in CA1 was ascribed to the transmission from CA3 to CA1.

Optical imaging of signal propagation from mossy fibers to CA1

To find mechanisms underlying the variations of the latencies, signal propagation from mossy fibers to CA1 was analyzed by optical recording in 14 slices. Optical images disclosed two distinct types of signal pathways from CA3 to CA1. These could be classified into fast and slow propagation according to latencies of optical signals recorded in CA1.

Fast propagation from CA3 and CA1

An example of the fast propagation is shown in Fig. 2. Images were obtained every 0.6 ms, but only every other image is shown in Fig. 2*A* for the sake of simplicity. In this case, the maximal change in the intensity of optical signals was 0.09% in the hilus and 0.06% in the stratum radiatum of CA1. Excitation was induced around the stimulating electrode in the hilus and spread to the stratum radiatum in the proximal part of CA3 within 1.2 ms (→ in 1.2-ms image, Fig. 2*A*). The signals then spread to the stratum radiatum (→ in 2.4-ms image) and oriens of CA3, expanded to cover the entire CA3 within 4.8 ms after stimulation (→ in 4.8-ms image), and then jumped to the stratum radiatum of the CA1 within 6 ms (→ in 6.0-ms image). Excitation reached the middle part of CA1 (∗ in 7.2-ms image) within 7.2 ms and spread over the entire CA1 by 10.8 ms. An optical signal in the fixed pixel at the stratum radiatum of CA1 (∗ in 7.2-ms image) is compared with the field potential at the corresponding area (the fast EPSP in Fig. 1*B*) in Fig. 2*B*. The optical signal and the field potential (Fig. 2*B*, *top* and *bottom traces*) had a good correlation in terms of their onset and initial slope. These results indicate that fast propagation observed by optical recording corresponds to the fast PSs group shown in Fig. 1.

The signals in the stratum oriens of CA3 were stronger and lasted longer than those in the stratum radiatum in this case, but not in all cases. In the pyramidal cell layers of CA3 and CA1, weak or no optical response was detected. When the optical responses shown in Fig. 2*A* were replayed in slow motion, the signals appeared to jump over the area between CA3 and CA1 and rapidly propagate through CA1. The optically silent region between CA3 and CA1 was identified as CA2 in the photograph of each slice.

Optical signals obtained from three pixels in the stratum radiatum of CA3, CA2, and the middle part of CA1 in the fast propagation are shown in Fig. 3*B*. The optical signal in CA3 (site labeled 1 in Fig. 3*A*) began at 3.0 ms and reached maximum amplitude by 4.2 ms (Fig. 3*B*, arrow A). No optical signal was detected in CA2 (site labeled 2 in Fig. 3*A*). The response in CA1 immediately followed that in CA3. The optical signal in the middle part of CA1 (site labeled 3 in Fig. 3*A*) reached maximum amplitude at 8.4 ms (Fig. 3*B*, arrow B). Optical signals in the stratum radiatum lasted for 30 ms, with a half-decay time of 10 ms in CA3 and for 20 ms in the middle part of CA1. After optical recording, careful electrical mapping in CA2 was performed but failed to detect the field potential despite distinct PSs in CA3 and CA1. In 8 of 14 slices, this pattern of the fast propagation was observed obviously.

Slow propagation from CA3 to CA1

In 6 of 14 slices, mossy fiber stimulation induced another pattern of propagation, which we call the slow propagation. In three of the six slices, only the slow propagation was detected. In the other three slices, a mixed pattern of the fast and slow propagation was observed.

An example of the slow propagation is shown in Fig. 4*A*. In brief, the signals spread into the middle part of CA1 (∗ in 10.8 ms-image) after 10.8 ms, almost 3.6 ms later than the fast propagation shown in Fig. 2*A*. As in the case of the fast propagation, the instantaneous activation around the stimulating electrode (Fig. 4*A*, → in 1.2-ms image) was followed within 2.4 ms by the activity in the strata radiatum and oriens of CA3 (→ in 2.4-ms image). Then optical signals gradually spread throughout the strata radiatum and lacunosum-moleculare of CA3 (→ in 4.8-ms image). A stronger signal was detected in DG than in the case of fast propagation. In this case, the maximal optical response in DG was 0.14%.

The slow propagation differed from the fast one in terms of the spatial and temporal patterns of optical signals occurring later than 6 ms. The most remarkable feature of the slow propagation was that the optical signals spread from CA3 into the area between CA3 and CA1 (Fig. 4*A*, → in 6-ms image). This area was identified as the CA2 region on the real image. The signal intensity gradually increased around this area until 9.6 ms after stimulation (→ in 7.2- and 8.4-ms images). At 9.6 ms, the proximal part of the stratum oriens (→ in 9.6-ms image) and the stratum radiatum of CA1 were activated simultaneously. An optical signal in the fixed pixel at the stratum radiatum (Fig. 4*A*, asterisk) is compared with the field potential at the corresponding area (slow EPSP in Fig. 1*B*) in Fig. 4*B*. The optical signal and the field potential (Fig. 4*B*, *top* and *bottom traces*) had a good correlation in terms of their onset and initial slope. These results indicate that the slow propagation observed by optical recording corresponds to the slow PS group shown in Fig. 1. When the slow propagation was replayed in slow motion, the signals were accumulated steadily in CA2 and flew abruptly to CA1.

Optical signals from three areas in the experiments of Fig. 4 are plotted in Fig. 3*C*. The optical signal in CA3 (site labeled 1 in Fig. 3*A*) started at 2.4 ms and reached maximum amplitude by 4.2 ms (Fig. 3*C*, arrow C), as in the case of fast propagation. The signal persisted in CA2 (site labeled 2 in Fig. 3*A*) before spreading into CA1 between 5.4 and 8.4 ms, although it was not detected in the fast propagation. The signal in the middle part of CA1 (site labeled 3 in Fig. 3*A*) gradually appeared around 7.0 ms and reached maximum amplitude between 11.4 and 12.6 ms (Fig. 3*C*, arrow D). The time difference between arrows B and D in Fig. 3 was 4.2 ms, which is consistent with the difference of latencies of the fast and the slow PSs.

Because such neuronal activity in CA2 had not been described previously, electrical recording was performed in CA2 after optical imaging of the slow propagation. Mossy fiber stimulation evoked PSs in CA2 with a latency of ~6.0–7.0 ms. They were similar in their time course to optical signals in CA2, which reached half-maximum amplitude after 6.6 ms (Fig. 3*C*).

DISCUSSION

In hippocampal slices obtained by transverse sectioning, synaptic connections between subregions are not fully pre-

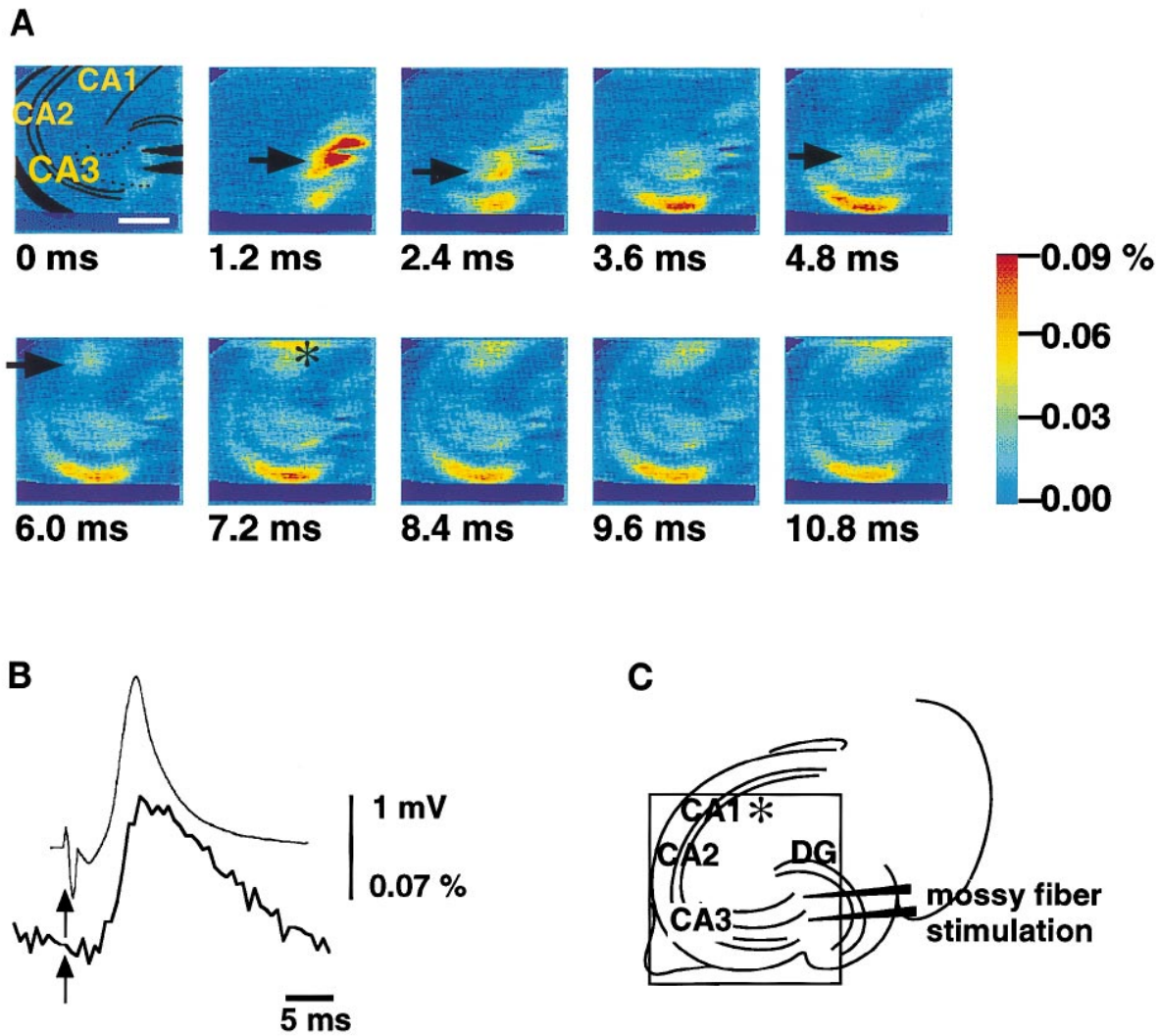

FIG. 2. Fast propagation of optical signals from mossy fibers to CA1 in a hippocampal slice. *A*: optical images obtained at times indicated. Mossy fibers were stimulated at 0 ms. Optical signals were expressed on a pseudocolor scale. Optical signals were induced instantaneously around stimulating electrode (→ in 1.2-ms image), spread over stratum radiatum of CA3 (→ in 2.4- and 4.8-ms images), invaded proximal part of CA1 (→ in 6.0-ms image), and then were transmitted to middle part of CA1 (∗ in 7.2-ms image). Scale bar in 0-ms image: 500 μm. Signals are transmitted from CA3 to CA1 without invading CA2. *B*: electrical (EPSP, *top trace*) and optical (*bottom trace*) signal obtained at middle part of CA1 (*C*, ∗). Electrical signal (EPSP) is from Fig. 1*B*, but its polarity is reversed. *C*: diagram showing hippocampal subregions and placement of stimulating and recording electrodes. Square: area of optical recording in *A*.

served (Brown and Zador 1990), because the ''lamellar'' organization of the classical trisynaptic circuit is oriented almost perpendicular to the alvear surface (Andersen et al. 1971). In fact, when a single CA3 pyramidal cell was labeled, its axon collaterals were found to terminate only rarely in CA1 within a transverse slice preparation (Ishizuka et al. 1990). Correspondingly, stimulation of single CA3 cells produces monosynaptic EPSPs in only 6% of CA1 pyramidal cells in transversely sectioned slices (Sayer et al. 1990). This is why stimulation of mossy fibers did not produce PSs in CA1 polysynaptically in transverse slices. In the present study, loss of polysynaptic connections was reduced by slicing the hippocampus along the alvear fibers. Especially when such slices were obtained from the middle part of the hippocampus, PSs were observed in CA1 in most cases. In those slices, we disclosed fast and slow signal propagations by both the electrical and optical recordings. CA2 neurons are signaling intermediates from CA3 to CA1 in the slow propagation, whereas the fast signals propagate along the well-known trisynaptic circuit.

Correlation between optical signals and changes in membrane potentials have been demonstrated in several studies (Albowitz and Kuhnt 1993; Tanifuji et al. 1997). Plenz and Aertsen (1993) have shown correspondence of optical signals with field EPSPs in CA1 of hippocampal slices. In the present study, a good correlation was obtained between optical signals and the field potentials of the stratum radiatum of CA1 in each case of the fast and slow propagations (Figs. 2*B* and 4*B*). Futhermore, several pharmacological manipulations affected the simultaneously recorded PSs and optical signals in the same way (Sekino, unpublished data). The only difference is that the optical signal could be detected longer than the field EPSPs. A similar observation has been reported in the piriform cortex in vitro (Sugitani

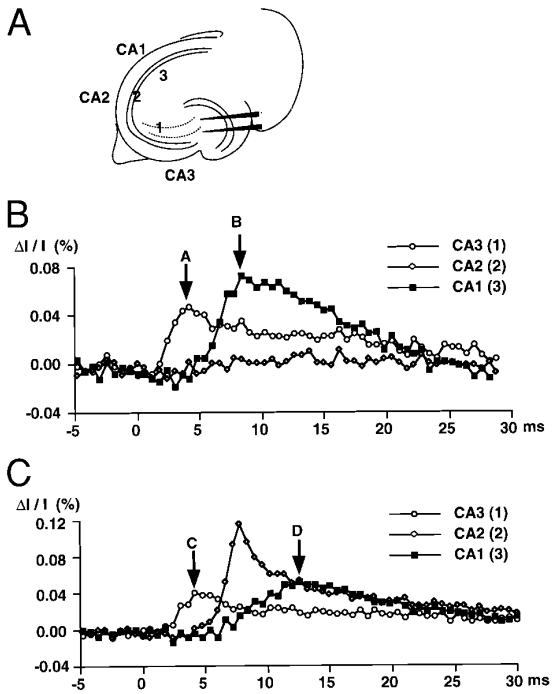

FIG. 3. Time course of optical signals of 3 areas. *A*: diagram showing position of a stimulating electrode in hilus and pixels located in stratum radiatum of CA3 (labeled 1), CA2 (part close to cell layer; labeled 2), and middle part of CA1 (labeled 3). *B* and *C*: % changes in light transmittance recorded in each pixel (ordinates) vs. time after mossy fiber stimulation (abscissas). Arrows: time required for signals to reach their maximal amplitude in CA3 and middle CA1. *B*: fast propagation. From data shown in Fig. 2. Delay between CA3 and CA1 activity, defined as time between the 2 arrows, was 4.2 ms. Note that no signal was detected in CA2. *C*: slow propagation. From data shown in Fig. 4. Delay between CA3 and CA1 activity was 8.4 ms. Note that a strong signal in CA2 precedes signal in CA1.

et al. 1994). This discrepancy can be expected because membrane depolarization, reflected by an optical signal, lasts longer than the synaptic current that produces a field EPSP (Kandel and Siegelbaum 1991).

We employed optical recording to find the origin of the delayed inputs to CA1, and found the additional pathway in which CA2 neurons are involved. The fast and slow propagations revealed by the optical imaging probably are the basis for the variation of latencies of PSs in CA1 and for the idea that part of polysynaptic inputs to CA1 neurons may originate from CA2 neurons.

Despite large PSs superimposed on EPSPs (Fig. 1*A*), only weak optical signals were obtained in the pyramidal cell layers of CA3 and CA1 (Figs. 2 and 4). Optical signals in the pyramidal cell layer are almost half that of those in the stratum radiatum in other studies (Grinvald et al. 1982; Plenz and Aertsen 1993). This discrepancy may have been due to the fact that the density of plasma membrane required for generation of optical signals is much lower in the cell body layer than in the stratum radiatum, which consists of a large number of dendrites and axons.

Patterns of mossy-fiber-induced fast and slow signal propagations from CA3 to CA1 are schematized in Fig. 5. In the fast propagation (Fig. 5*A*), CA1 is excited immediately after CA3. This is probably mediated by the Schaffer collateral inputs. Absence of optical signals in CA2 corresponds to absence of electrical responses in this area. Action potentials of CA3 axons should propagate through CA2 to CA1 even in the fast propagation, but they might be asynchronous and too small to be detected. Actually, the PSs or field EPSPs in CA1 are not preceded by a presynaptic volley of the Schaffer collateral (Fig. 1, *A* and *B*). The fact that fast propagation was observed in 11 of 14 slices obtained by oblique sectioning indicates that the Schaffer collateral–CA1 connection is more dominantly distributed along this plane than the delayed pathway via CA2.

In the slow propagation (Fig. 5*B*), signals accumulated in CA2 and then spread to CA1. Optical signals traveled along not only the stratum radiatum but also the stratum oriens of CA1. Tamamaki et al. (1988) have shown that horseradish-peroxidase-loaded pyramidal neurons in CA2 and CA3a project to both the stratum radiatum and the stratum oriens of CA1 along the alveus. Therefore we conclude that CA2 neurons mediate slow transmission from CA3 to CA1. However, involvement of the adjacent parts of CA3a and CA1 cannot be excluded, because of the limit of the spatial resolution of the detector used in the present study.

Most mossy fibers terminate in CA3 and do not reach CA2 (Ishizuka et al. 1990; Lorente de Nó 1934), but CA2 is considered to resemble CA3 in terms of intrahippocampal connections (Amaral and Witter 1995). Several authors (Bernard and Wheal 1994; Lopes Da Silva et al. 1990) included CA2 in the most distal part of CA3. Unique features of CA2 have been demonstrated, however. After application of penicillin or bicuculline to hippocampal slices, stimulation of mossy fibers produces a synchronized burst discharge in CA2 neurons (Wong and Traub 1983). This suggests involvement of CA2 in generation of epileptic discharges. Immunohistochemically, CA2 is distinguished from other regions (Woodhams et al. 1993) by intensive expression of basic fibroblast growth factor (Matsuyama et al. 1992), neurotrophin-3 (Wetmore and Olson 1993), and extracellular matrix molecules (Célio 1993). Nevertheless, whether CA2 neurons can play a specific role in the hippocampus continues to be a topic for debate. In the present study, we first demonstrated that CA2 neurons activate CA1 neurons as excitatory interneurons between CA3 and CA1.

Detection of both fast and slow propagations in the same slices indicates the coexistence of two mechanisms of propagation. However, this coactivation was observed only in 3 of 14 slices. This suggests that the angle of the plane for the slow propagation is a little different from that for the fast propagation.

Considering the physiological role of the CA2 activity, the CA2-CA1 connection could act as a modulatory circuit for activities of CA1 neurons. When CA1 neurons receive enough monosynaptic inputs from CA3 neurons to generate fast action potentials, the delayed inputs from CA2 would not contribute to the spikes. The inputs would prolong EPSPs in CA1 and influence succeeding responses. When the CA1 neurons receive subthreshold inputs directly from CA3 neurons, inputs from CA2 would generate the delayed action potential. In a mixed pattern of the fast and slow propagations, timing of action potentials would distribute among fast and slow latencies.

We suppose that extensive activation of CA3 is needed for slow propagation, because strong excitation of DG and/or the stratum lacunosum-moleculare of CA3 was observed in most cases of slow propagation. Application of picrotoxin or 8-cyclo-

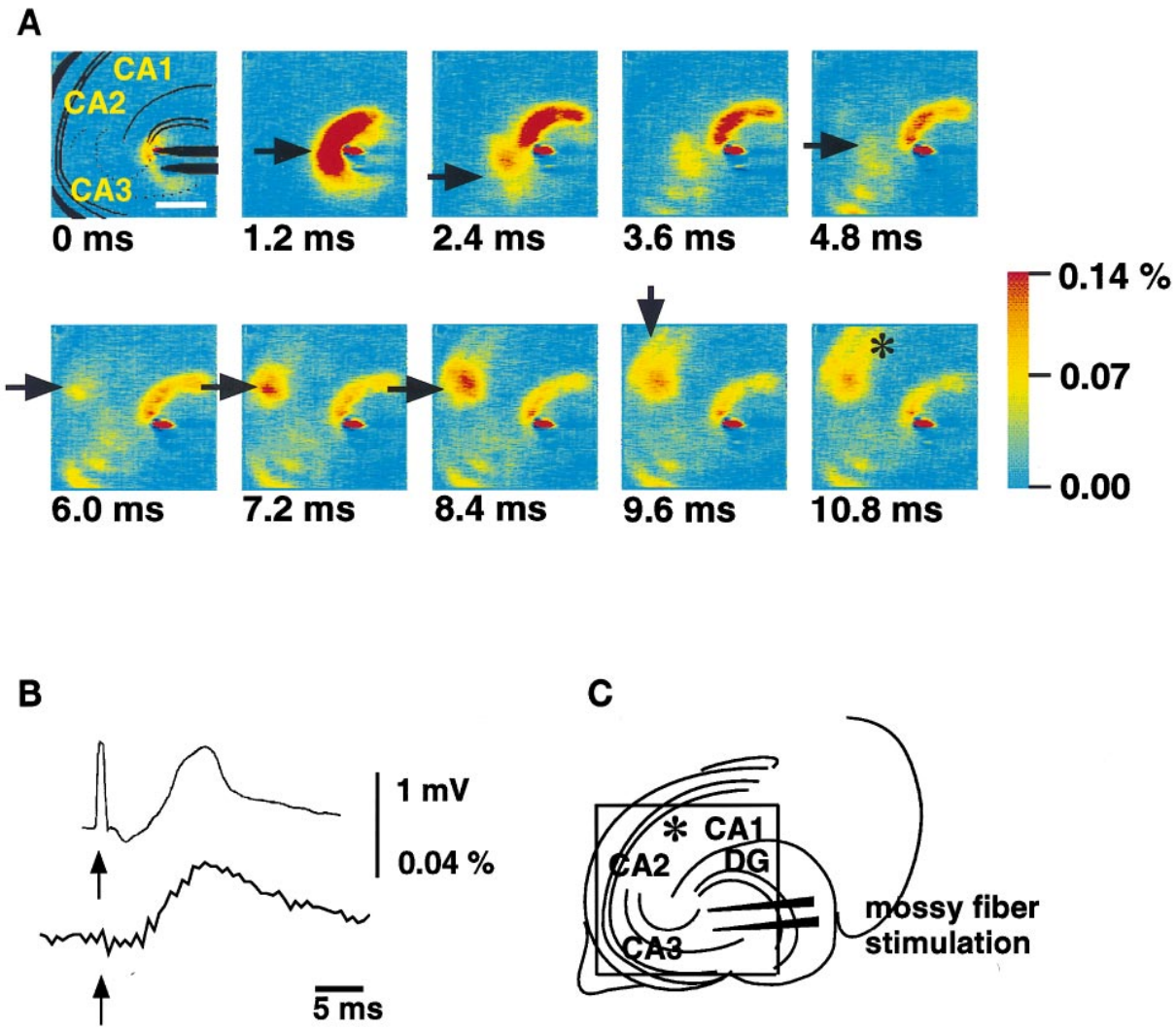

FIG. 4. Slow propagation of optical signals from CA3 to CA1 in a hippocampal slice. *A*: optical images obtained at times indicated. Mossy fibers were stimulated at 0 ms. Optical signals were induced instantaneously around stimulating electrode (→ in 1.2-ms image), spread over stratum radiatum of CA3 (→ in 2.4- and 4.8-ms images), invaded CA2 (→ in 6.0-, 7.2-, and 8.4-ms images), and then were transmitted to stratum oriens (→ in 9.6-ms image) and stratum radiatum of CA1. Asterisk in 10.8-ms image: middle part of CA1. Scale bar in 0-ms image: 500 μm. *B*: electrical (EPSP, *top trace*) and optical (*bottom trace*) signal obtained at middle part of CA1 (*C*, asterisk). EPSP is from Fig. 1*B*, but its polarity is reversed. *C*: diagram showing hippocampal subregions and placement of stimulating and recording electrodes. Square: area of optical recording in *A*.

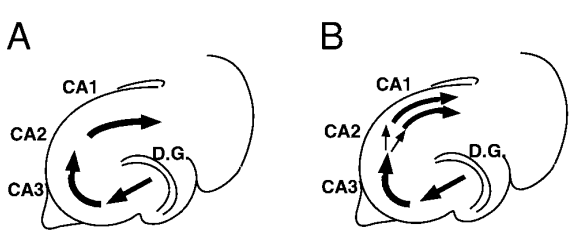

FIG. 5. Schematic drawings of 2 types of activity propagation following mossy fiber stimulation in hippocampal slices. *A*: fast propagation through a monosynaptic connection between CA3 and CA1. *B*: slow propagation from CA3 to CA1 involves CA2 activation. Activity is propagated simultaneously in stratum oriens and stratum radiatum of CA1.

pentyl-theophylline induced CA2 activities in slices in which activation of this region had not been detected previously (Sekino and Obata, unpublished data). These results suggest that slow propagation is induced by extensive synaptic inputs to CA2 neurons and is subject to γ-aminobutyric acid- and adenosine-mediated inhibition of synaptic transmission. CA3 pyramidal cells and some interneurons in CA3 and in the hilus may innervate CA2. Actually, CA2 is the principal target of the supramamillary nucleus (Haglund et al. 1984; Maglóczky et al. 1994). Neuronal activity in CA2 is likely to be controlled by extrahippocampal areas in vivo. Thus synaptic integration within CA2 might act as a modulator between CA3 and CA1 for delayed information transfer.

The distribution of synaptic connections between CA3 and CA1 neurons is not exclusively lamellar, and association fibers of CA3 and CA2 cells have been traced over a long distance across the septotemporal axis (Amaral and Witter 1989; Ishizuka et al. 1990; Lorente de Nó 1934; Tamamaki et al. 1988). These facts suggest that CA2 is involved in information flow along not only a lamellar plane but also the longitudinal axis of the hippocampal formation.

In conclusion, the signal propagation via CA2 should be taken into consideration in the network analysis of hippocampal function.

We thank Dr. N. Tamamaki for comments on this study and Drs. G. Augustine, T. Shirao, and C. Aoki for critical readings of this manuscript.

This work was supported in part by Ministry of Education Grants-in-Aid 05858121 to Y. Sekino and 04454142 and 07279107 to K. Obata.

Present address of M. Tanifuji: Laboratory for Integrative Neural System, Frontier Research Program, The Institute of Physical and Chemical Research (RIKEN), Wako-shi, Saitama 351-01, Japan.

Address for reprint requests: Y. Sekino, Dept. of Neurobiology and Behavior, Gunma University School of Medicine, Showa-machi, Maebashi 371, Japan.

Received 28 August 1995; accepted in final form 14 March 1997.

REFERENCES

ALBOWITZ, B. AND KUHNT, U. Evoked changes of membrane potential in guinea pig sensory neocortical slices: an analysis with voltage-sensitive dyes and a fast optical recording method. *Exp. Brain Res.* 93: 213–225, 1993.

ALGER, B. E. AND TEYLER, T. J. Long-term and short-term plasticity in the CA1, CA3 and dentate regions of the rat hippocampal slice. *Brain Res.* 110: 463–480, 1976.

AMARAL, D. G. AND WITTER, M. P. The three-dimensional organization of the hippocampal formation: a review of anatomical data. *Neuroscience* 31: 571–591, 1989.

AMARAL, D. G. AND WITTER, M. P. Hippocampus. In: *The Rat Nervous System* (2nd ed.), edited by G. Paxinos. San Diego, CA: Academic, 1995, p. 460–467.

ANDERSEN, P., BLISS, T.V.P., AND SKREDE, K. K. Lamellar organization of hippocampal excitatory pathways. *Exp. Brain Res.* 13: 222–238, 1971.

BERNARD, C. AND WHEAL, H. V. Model of local connectivity patterns in CA3 and CA1 areas of the hippocampus. *Hippocampus* 4: 497–529, 1994.

BLISS, T.V.P. AND COLLINGRIDGE, G. L. A synaptic model of memory: long-term potentiation in the hippocampus. *Nature* 361: 31–39, 1993.

BROWN, T. H. AND ZADOR, A. M. Hippocampus. In: *The Synaptic Organization of the Brain* (3rd ed.), edited by G. M. Shepherd. Oxford, UK: Oxford Univ. Press, 1990, p. 347–388.

CÉLIO, M. Perineuronal nets of extracellular matrix around parvalbumin-containing neurons of the hippocampus. *Hippocampus* 3: 55–60, 1993.

CINELLI, A. R. AND KAUER, J. S. Voltage-sensitive dyes and functional activity in the olfactory pathway. *Annu. Rev. Neurosci.* 15: 321–351, 1992.

GRINVALD, A., COHEN, L. B., LESHER, S., AND BOYLE, M. B. Simultaneous optical monitoring of activity of many neurons in invertebrate ganglia using a 124-element photodiode array. *J. Neurophysiol.* 45: 829–840, 1981.

GRINVALD, A., HILDESHEIM, R., GUPTA, R., AND COHEN, L. B. Better fluorescent probes for optical measurement of changes in membrane potential (Abstract). *Biol. Bull. Woods Hole* 159: 484, 1980.

GRINVALD, A., MANKER, A., AND SEGAL, M. Visualization of the spread of electrical activity in rat hippocampal slices by voltage-sensitive optical probes. *J. Physiol. (Lond.)* 333: 269–291, 1982.

HAGLUND, L., SWANSON, L. W., AND KÖHLER, C. The projection of the supramammillary nucleus to the hippocampal formation: an immunohistochemical and anterograde transport study with the lectin PHA-L in the rat. *J. Comp. Neurol.* 229: 171–185, 1984.

HAUG, F. S. Light microscopical mapping of the hippocampal region, the pyriform cortex and the corticomedial amygdaloid nuclei of the rat with Timm's sulphide silver method. I. Area dentata, hippocampus and subiculum. *Z. Anat. Entwicklungsgesch.* 145: 1–27, 1974.

ICHIKAWA, M., IIJIMA, T., AND MATSUMOTO, G. Real-time optical recording of neuronal activities in the brain. In: *Brain Mechanisms of Perception and Memory*, edited by T. Ono, L. R. Squire, M. E. Raichle, D. I. Perrett, and M. Fukuda. Oxford, UK: Oxford Univ. Press, 1993, p. 638–648.

IIJIMA, T., WITTER, M. P., ICHIKAWA, M., TOMINAGA, T., KAJIWARA, R., AND MATSUMOTO, G. Entorhinal-hippocampal interactions revealed by real-time imaging. *Science* 272: 1176–1179, 1996.

ISHIZUKA, N., WEBER, J., AND AMARAL, D. G. Organization of intrahippocampal projections originating from CA3 pyramidal cells in the rat. *J. Comp. Neurol.* 295: 580–623, 1990.

KANDEL, E. R. AND SIEGELBAUM, S. A. Directly gated transmission at the nerve-muscle synapse. In: *Principles of Neural Science* (3rd ed.), edited by E. R. Kandel, J. H. Schwartz, and T. M. Jessell. East Norwalk, CT: Appleton & Lange, 1991, p. 149–152.

KONNERTH, A., OBAID, A. L., AND SALZBERG, B. M. Optical recording of electrical activity from parallel fibres and other cell types in skate cerebellar slices in vitro. *J. Physiol. (Lond.)* 393: 681–702, 1987.

LOPES DA SILVA, F. H., WITTER, M. P., BOEIJINGA, P. H., AND LOHMAN, A.H.M. Anatomic organization and physiology of the limbic cortex. *Physiol. Rev.* 70: 453–511, 1990.

LORENTE DE NÓ, R. Studies on the structure of the cerebral cortex. II. Continuation of the study of the ammonic system. *J. Psychol. Neurol.* 46: 113–177, 1934.

MAGLÓCZKY, Z., ACSÁDY, L., AND FREUND, T. F. Principal cells are the postsynaptic targets of supramammillary afferents in the hippocampus of the rat. *Hippocampus* 4: 322–334, 1994.

MATSUYAMA, A., IWATA, H., OKUMURA, N., YOSHIDA, S., IMAIZUMI, K., LEE, Y., SHIRAISHI, S., AND SHIOSAKA, S. Localization of basic fibroblast growth factor-like immunoreactivity in the rat brain. *Brain Res.* 587: 49–65, 1992.

PLENZ, D. AND AERTSEN, A. Current source density profiles of optical recording maps: a new approach to the analysis of spatio-temporal neural activity patterns. *Eur. J. Neurosci.* 5: 437–448, 1993.

SAYER, R. J., FRIEDLANDER, M. J., AND REDMAN, S. J. The time course and amplitude of EPSPs evoked at synapses between pairs of CA3/CA1 neurons in the hippocampal slice. *J. Neurosci.* 10: 826–836, 1990.

SCHWARTZKROIN, P. A. AND WESTER, K. Long-lasting facilitation of a synaptic potential following tetanization in the in vitro hippocampal slice. *Brain Res.* 89: 107–119, 1975.

SCOVILLE, W. B. AND MILNER, B. Loss of recent memory after bilateral hippocampal lesions. *J. Neurol. Neurosurg. Psychiatry* 20: 11–21, 1957.

SUGITANI, M., SUGAI, T., TANIFUJI, M., MURASE, K., AND ONODA, N. Optical imaging of the in vitro guinea pig piriform cortex activity using a voltage-sensitive dye. *Neurosci. Lett.* 165: 215–218, 1994.

TAMAMAKI, N., ABE, K., AND NOJYO, Y. Three-dimensional analysis of the whole axonal arbors originating from single CA2 pyramidal neurons in the rat hippocampus with the aid of a computer graphic technique. *Brain Res.* 452: 255–272, 1988.

TANIFUJI, M., SUGIYAMA, T., AND MURASE, K. Horizontal propagation of excitation in rat visual cortical slices revealed by optical imaging. *Science* 266: 1057–1059, 1994.

TANIFUJI, M., YAMANAKA, A., SUNABA, R., TERAKAWA, S., AND TOYAMA, K. Optical responses evoked by white matter stimulation in rat visual cortical slices and their relation to neural activities. *Brain Res.* 738: 83–95, 1997.

WETMORE, C. AND OLSON, L. Expression and regulation of neurotrophins and their receptors in hippocampal systems. *Hippocampus* 3: 171–182, 1993.

WONG, R.K.S. AND TRAUB, R. D. Synchronized burst discharge in disinhibited hippocampal slice. I. Initiation in CA2–CA3 region. *J. Neurophysiol.* 49: 442–458, 1983.

WOODHAMS, P. L., CELIO, M. R., ULFIG, N., AND WITTER, M. P. Morphological and functional correlates of borders in the entorhinal cortex and hippocampus. *Hippocampus* 3: 303–312, 1993.

ZOLA-MORGAN, S. M. AND SQUIRE, L. R. The primate hippocampal formation: evidence for a time-limited role in memory storage. *Science* 250: 288–290, 1990.

ZOLA-MORGAN, S., SQUIRE, L. R., AND AMARAL, D. G. Human amnesia and the medial temporal region: enduring memory impairment following a bilateral lesion limited to field CA1 of the hippocampus. *J. Neurosci.* 6: 2950–2967, 1986.